

Article

Theoretical Impact of Manufacturing Tolerance on Lithium-Ion Electrode and Cell Physical Properties

William Yourey 

College of Engineering, Penn State University—Hazleton Campus, Hazleton, PA 18202, USA; wxy40@psu.edu

Received: 18 March 2020; Accepted: 8 April 2020; Published: 15 April 2020



Abstract: The range of electrode porosity, electrode internal void volume, cell capacity, and capacity ratio that result from electrode coating and calendering tolerance can play a considerable role in cell-to-cell and lot-to-lot performance variation. Based on a coating loading tolerance of $\pm 0.4 \text{ mg/cm}^2$ and calender tolerance of $\pm 3.0 \mu\text{m}$, the resulting theoretical range of physical properties was investigated. For a target positive electrode porosity of 30%, the resulting porosity can range from 19.6% to 38.6%. To account for this variation during the manufacturing process, as much as 41% excess or as little as 59% of the target electrolyte quantity should be added to cells to match the positive electrode void volume. Similar results are reported for a negative electrode of 40% target porosity, where a range from 30.8% to 48.0% porosity is possible. For the negative electrode as little as 72% up to 28% excess electrolyte should be added to fill the internal void space. Although the results are specific to each electrode composition, density, chemistry, and loading the presented process highlight the possible variability of the produced parts. These results are further magnified as cell design moves toward higher power applications with thinner electrode coatings.

Keywords: porosity; manufacturing; tolerance; Lithium-Ion; capacity ratio; electrolyte volume

1. Introduction

Lithium ion cells have been the pinnacle method of providing energy for portable electronics, with numerous manufacturers around the world providing batteries of different chemistries [1], dimensions, capacity [2], and power [3]. With numerous positive electrode active materials available to cell manufactures, lithium cobalt dioxide (LiCoO_2) has historically been the material of choice due to its proven performance and reliability [4,5]. In manufacturing LiCoO_2 cells at both the commercial and laboratory scale, variability is introduced. These tolerances on produced parts, present during any manufacturing process, can have a large impact on the final product's reliability, repeatability, and functionality. Lithium ion cells are no exception to this and thus, manufacturing variation must be considered during cell performance evaluations [6]. Whether it be the formed aluminum laminate package dimensions for prismatic cells, electrode dimensions, electrode coating mass loading, or electrode calender thickness, as well as other production steps, these variations inevitably affect the final product [7]. Numerous authors have indirectly investigated the impact of these manufacturing tolerances on cell performance. Investigating the effect of both anode and cathode porosity on thick lithium ion electrodes, Singh et al. [8] demonstrated that variation in cathode and anode porosity for a constant heavy loading play a considerable role in cell performance, effecting both electrode integrity and cell rate capability, while also concluding that peak performance occurs at an electrode specific target porosity, where small deviations effect performance. The effect of anode porosity and thickness on capacity fade was investigated by Suthar et al. [9], where low porosity yields high electrode tortuosity, a significant reduction in rate capability, and increased capacity fade. The influence of positive [10], and negative [11] electrode density was demonstrated to show that as electrode density is increased, internal electrode electrolyte volume is decreased, leading to increased polarization and

poor high rate performance, as well as influencing irreversible capacity loss during formation [12]. The effect of a negative to positive electrode matching ratio on various performance characteristics have also been investigated, showing the effect of area ratio [13], mass ratio [14], and areal capacity ratio [15], and concluding that maintaining an optimal ratio (mass or capacity) is critical to performance, and small deviations result in possible lithium metal plating or increased irreversible capacity loss. Authors have also shown the effects of electrolyte volume on cell performance as a function of electrolyte to electrode void volume [16,17], highlighting the critical importance of sufficient electrolyte volume to cell performance. It is the author's goal to look at the resulting electrode and cell physical properties, namely electrode porosity, change in electrode internal void volume, and capacity ratio that result as a function of electrode coating and calendering tolerance. These tolerances and resulting physical property variations have a direct effect on the resulting cell capacity, rate capability, and cycle life and should be considered during the cell design and evaluation process.

As electrode coating and calendering are performed through various techniques, from laboratory scale doctor-blading to large commercial scale web coating, a relatively large tolerance was used for the evaluated electrode coating ($\pm 0.4 \text{ mg/cm}^2$) and calendering process ($\pm 3.0 \mu\text{m}$). Regardless of technique and scale, variation is present in each process [18].

For lab scale electrochemical analysis, coin cells are primarily used as these cells are a quick and cost-effective method to acquire electrochemical results, compared to more elaborate, typically more reproducible, lithium ion pouch or hardware cells. Coin cells have the additional advantage of containing a relatively large void volume inside the crimped cell and outside the typical single pair electrode stack [16]. This additional space allows for an excess of electrolyte to be added, ensuring adequate volume and proper electrode wetting. For analysis purpose, the electrode porosity change would be more critical compared to the change in electrolyte volume which should be added for full electrode saturation, as this porosity change affects cell performance [9,10]. During the manufacturing of lithium ion pouch cells for commercial applications, the void volume outside the electrode stack is minimized, with the goal of producing a cell or battery with the greatest volumetric energy density possible. The idea of maximizing cell volumetric energy density, while still containing enough void space for electrolyte, is no trivial matter, especially when taking into account the large variations in stack void volume that occur during the manufacturing process based on coating and calendering tolerance.

Relating to the variations of electrode and cell physical parameters resulting from manufacturing tolerances, the following theoretical results are provided for single positive and negative electrode coatings absent of foil. The methods and process presented, through small alterations, can be applied to both single and double side-coated foils of any thickness, as well as supercapacitor electrode manufacturing [19]. Various coating methods, drying procedures, binder types, active materials, and calender methods all affect electrode "spring back" or relaxation following electrode processing. Due to the numerous calendering, coating, and composition options available, as well as alternative non-commercial electrode materials under development [20], this has been omitted. For this case study, one pair of lithium ion electrode compositions at three loadings have been selected as representative cells. With these representing a high-energy, standard, and high-power mass loading, this selection is an attempt to replicate commercial lithium ion cells in production today, where the focus of the manuscript is to provide a possible explanation into lot-to-lot variation which occurs in cells where all manufactured parts meet design specifications and tolerances. The resulting large range of porosity and cell matching ratio can account for this variation. The presented results are scalable for any coating formulation, thickness, electrode size, and capacity ratio, with the goal being to highlight the considerations which should be investigated during the design and manufacturing process and the large impact of process variation. Through an extensive literature review, the author has found no similar work published, including one where both electrode coating and calendering variations are considered. Two processes are present in all lithium ion electrodes manufactured commercially today.

2. Materials and Methods

Generic or standard LiCoO₂ positive electrode and graphite negative electrode formulation were selected for the investigation of manufacturing tolerance on electrode and cell physical characteristics, namely porosity, cell capacity, matching ratio, and void volume. Table 1 highlights the formulations used for both positive and negative electrodes along with the resulting mixture density used in determining the target electrode calender thickness. The selected formulations, required for analysis, can be altered to any desired formulation and evaluation.

Table 1. Generic positive and negative electrode formulations.

Positive Electrode		
Material	Weight Percent	Density (g/cm ³)
LiCoO ₂	93	5.00
Conductive Additive	4	2.00
PVDF Electrode Binder	3	1.80
Positive Mixture	-	4.49
Negative Electrode		
Material	Weight Percent	Density (g/cm ³)
Active Carbon	92	2.20
Conductive Additive	1	2.00
PVDF Electrode Binder	7	1.80
Negative Mixture	-	2.16

Three different electrode coating weights or loadings (mg/cm²) were used to highlight the effect manufacturing tolerances have on the resulting electrode and cell physical properties. Using a positive electrode specific capacity of 150 mAh/g for LiCoO₂ (4.2 V vs. Graphite), the three selected loadings correspond to a high power/low energy, mid-range, and high energy/low power loading of 1.40, 2.79 and 4.19 mAh/cm², respectively. This range of electrode loadings was selected as it represents the range of the majority of coatings used in commercial lithium ion cells today and are displayed in Table 2 [21].

Table 2. Target positive electrode loadings and corresponding areal capacity.

Design	Electrode Loading	LiCoO ₂ Loading	mAh/cm ² @ 150 mAh/g
High Power: Low Energy	10 mg/cm ²	9.3 mg/cm ²	1.40
Mid-Range	20 mg/cm ²	18.6 mg/cm ²	2.79
High Energy: Low Power	30 mg/cm ²	27.9 mg/cm ²	4.19

The amount of negative electrode active material present in a lithium ion cell must correctly match lithium content in the positive electrode for a specific charge voltage. This results in a favorable negative to positive equal area active material capacity ratio. Table 3 illustrates the corresponding negative electrode loadings used to match the previously outlined positive electrodes from Table 2. The weight ratios of positive to negative active components are shown along with the areal capacity loading of the active graphite. The areal loading represents a 300 mAh/g reversible capacity negative electrode material. Also shown is the reversible capacity ratio of the negative and positive electrode, assuming 300 and 150 mAh/g, respectively.

Table 3. Negative electrode loadings and corresponding areal capacity, Positive to negative active material weight ratio, and reversible capacity ratio (graphite = 300 mAh/g and LiCoO₂ = 150 mAh/g).

Design	Electrode Loading	Graphite Loading	mAh/cm ² @ 300 mAh/g	P:N Active Weight Ratio	N:P Capacity Ratio
High Power	5.56 mg/cm ²	5.12 mg/cm ²	1.53	1.82:1.00	1.1:1.0
Mid-Range	11.12 mg/cm ²	10.23 mg/cm ²	3.07	1.82:1.00	1.1:1.0
High Energy	16.68 mg/cm ²	15.35 mg/cm ²	4.60	1.82:1.00	1.1:1.0

Given the electrode target loadings, material density and target porosity, the corresponding calender density and target calender thickness can be calculated from Equations (1) and (2), where rho, ρ , represents density.

$$\text{Calender } \rho = (\text{Material } \rho) \times (1 - \text{porosity}) \quad (1)$$

$$\text{Calender Thickness (cm)} = (\text{Electrode Loading (g cm}^{-2}\text{)} \times (\text{Calender } \rho \text{ (g cm}^{-3}\text{)})^{-1} \quad (2)$$

The following results are compared to a target calender thickness for both the positive and negative electrodes for each cell design. Variation in electrode loading, during the coating process and calendering to a target thickness, will result in a range of cell capacity, electrode capacity ratio, and electrode porosity. The resulting variation in electrode porosity from the nominal design results in a range of electrode void volume. For optimal cell performance, this electrode internal void volume should be saturated with electrolyte during the electrolyte addition step of the manufacturing process. Saturation ensures proper cell function and safety during subsequent cycling and evaluation.

Using an electrode coating tolerance of $\pm 0.4 \text{ mg/cm}^2$ and a calender tolerance of $\pm 3.0 \mu\text{m}$, analysis was performed to determine the possible range in electrode porosity and the resulting variation in positive and negative electrode void volume. The corresponding electrolyte volume changes required to fully saturate the lithium ion electrodes, cell capacity change, and negative to positive capacity ratio change are also presented. Combining the tolerances of the loading and calender process, the range of electrode porosity can be calculated from Equation (3), and from this the electrode void volume can be calculated for any electrode size.

$$\text{Porosity} = 1 - x/y \quad (3)$$

where $x = \text{Target Electrode Loading} \pm \text{Loading Tolerance (g cm}^{-2}\text{)}$, $y = \text{Electrode } \rho \text{ (g cm}^{-3}\text{)} \times \text{Target Calender Thickness} \pm \text{Calender Tolerance (cm)}$.

3. Results and Discussion

3.1. Effect of Electrode Calendering Tolerance

With the assumption that during the coating process the target positive and negative electrodes loadings are correct, the resulting cell should possess the correct negative to positive capacity ratio per the design specifications. Focusing solely on the impact calender tolerance will have on electrode porosity for the three previously highlighted positive and negative electrode loadings, as expected, it can be seen in Figure 1 that the largest impact occurs for the lightest electrode loading. The target electrode calender thickness for these high power/low energy electrodes is the thinnest of the three designs. With these lighter electrode loadings, if the electrode is calendered to a thinner value than the target, a larger percentage of the porosity is removed, or vice versa, for a higher value than target calender thickness.

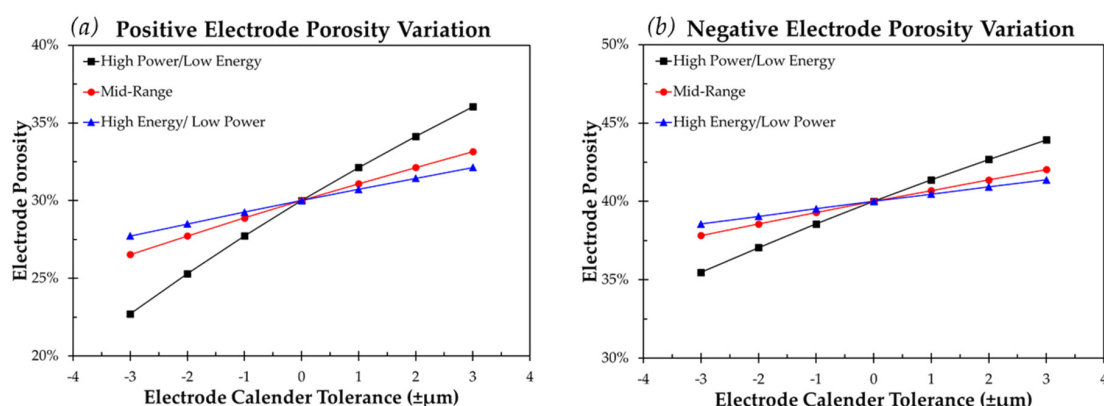


Figure 1. Variation in (a) positive electrode porosity and (b) negative electrode porosity for a calender tolerance range of $\pm 3.0 \mu\text{m}$ and a target porosity of 30% and 40% respectively.

The porosity range highlighted in Figure 1 for a thin, high power, low energy electrode translates to 22.7–36.0% for a positive electrode and 35.5–43.9% for a negative electrode with target values of 30% and 40%, respectively. Although the internal electrode void volume change per area from the target porosity is equal across all cell and electrode types for the same calender tolerance, when adding electrolyte to a cell the percent less or excess electrolyte required to account for this variation is a critical number to consider. Table 4 demonstrates the percent change in electrode internal void volume resulting from variation in electrode calender thickness.

Table 4. Percent change in electrode void volume resulting from electrode calendering tolerance.

Design	Calender Range from Target Value (μm)						
	-3	-2	-1	0	1	2	3
Low Energy (Positive)	-31.4%	-21.0%	-10.5%	0.0%	10.5%	21.0%	31.4%
Low Energy (Negative)	-17.5%	-11.7%	-5.8%	0.0%	5.8%	11.7%	17.5%
Mid-Range (Positive)	-15.7%	-10.5%	-5.2%	0.0%	5.2%	10.5%	15.7%
Mid-Range (Negative)	-8.8%	-5.8%	-2.9%	0.0%	2.9%	5.8%	8.8%
High Energy (Positive)	-10.5%	-7.0%	-3.5%	0.0%	3.5%	7.0%	10.5%
High Energy (Negative)	-5.8%	-3.9%	-1.9%	0.0%	1.9%	3.9%	5.8%

For the data presented in Table 4, the importance and impact of electrode design can be noted. Electrodes with a lower composite density (negative electrodes) see a smaller change in internal void volume for the same variation in calender thickness. Also attributing to this effect is the chosen target porosity of the electrode. A higher target porosity sees a smaller change in electrode void volume percentage as electrode calender thickness is changed. As cell designs move toward higher energy density, either through reduced porosity or increased active material content, this effect is magnified, and consideration becomes increasingly vital.

3.2. Effect of Electrode Coating Tolerance

Similar to the effect of calender variation described in Section 3.1, analysis was performed with electrode coating tolerance. For the following results, a coating tolerance of $\pm 0.4 \text{ mg/cm}^2$ is applied to determine the impact on not only electrode porosity and void volume, but also capacity and cell capacity ratio. As typical commercial lithium ion cells are designed with excess negative electrode material acting as a safety factor to eliminate lithium plating, variation from the target coating (mg/cm^2) directly affects the mass of the active material. This results in variation of the negative to positive capacity ratio along with cell capacity. Table 5 represents the negative to positive capacity ratio for a coating tolerance of $\pm 0.4 \text{ mg/cm}^2$. These following results are shown for a high power-low energy electrode pair, as this low mass loading shows the largest range of capacity ratio of the three.

Table 5. Variation in negative to positive equal area capacity ratio resulting from an electrode coating tolerance of $\pm 0.4 \text{ mg/cm}^2$.

High Power/Low Energy	Negative Electrode Coating (mg/cm^2)									
	Pos. Electrode (mg/cm^2)	-0.4	-0.3	-0.2	-0.1	0.0	0.1	0.2	0.3	0.4
-0.4		1.06	1.08	1.10	1.13	1.15	1.17	1.19	1.21	1.23
-0.3		1.05	1.07	1.09	1.11	1.13	1.15	1.17	1.20	1.22
-0.2		1.04	1.06	1.08	1.10	1.12	1.14	1.16	1.18	1.20
-0.1		1.03	1.05	1.07	1.09	1.11	1.13	1.15	1.17	1.19
0.0		1.02	1.04	1.06	1.08	1.10	1.12	1.14	1.16	1.18
0.1		1.01	1.03	1.05	1.07	1.09	1.11	1.13	1.15	1.17
0.2		1.00	1.02	1.04	1.06	1.08	1.10	1.12	1.14	1.16
0.3		0.99	1.01	1.03	1.05	1.07	1.09	1.11	1.13	1.14
0.4		0.98	1.00	1.02	1.04	1.06	1.08	1.10	1.11	1.13

The negative to positive capacity ratios range from 0.98 to 1.23, 1.04 to 1.16, and 1.06 to 1.14 for high power/low energy, mid-range, and low power/high energy coatings, respectively, again highlighting that as thinner, higher active material content loadings are utilized, the impact of manufacturing tolerance is magnified. For a higher power electrode, the target loading is a lower value; with the same coating tolerance applied to all coatings, the lightest loadings see the largest impact of coating variation.

Electrodes calendered to the correct thickness still demonstrate a range of porosity resulting from loading variation. Figure 2 and Table 6 represent both the range of porosity as well as the percent change in electrode void volume. These results are provided for a positive and negative electrode calendered to the target thickness.

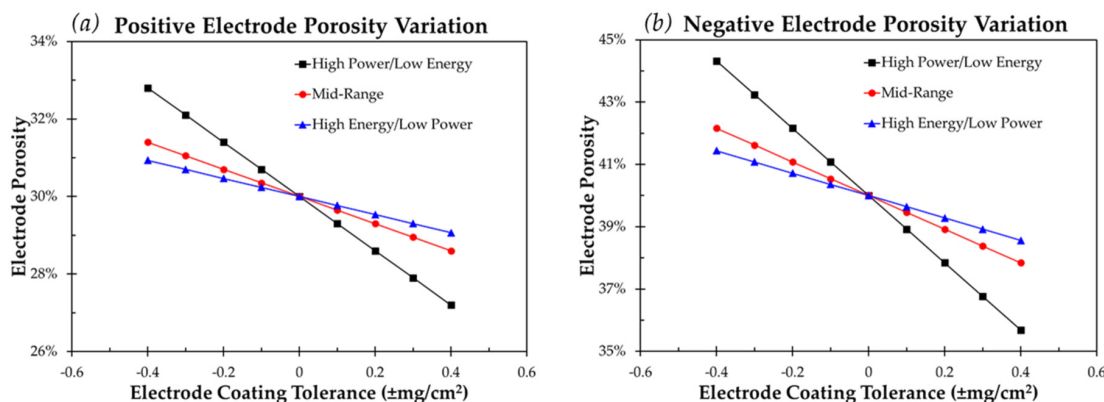


Figure 2. Variation in (a) positive electrode porosity and (b) negative electrode porosity for a coating tolerance of $\pm 0.4 \text{ mg}/\text{cm}^2$ and a target porosity of 30% and 40%, respectively.

Table 6. Percent change in electrode void volume resulting from electrode loading tolerance.

Electrode Loading	Electrode Percent Internal Void Volume Change								
	Electrode Loading Range from Target Value (mg/cm^2)								
	-0.4	-0.3	-0.2	-0.1	0	0.1	0.2	0.3	0.4
Low Energy (Positive)	9.33%	7.00%	4.67%	2.33%	0.00%	-2.33%	-4.67%	-7.00%	-9.33%
Low Energy (Negative)	10.79%	8.09%	5.40%	2.70%	0.00%	-2.70%	-5.40%	-8.09%	-10.79%
Mid-Range (Positive)	4.67%	3.50%	2.33%	1.17%	0.00%	-1.17%	-2.33%	-3.50%	-4.67%
Mid-Range (Negative)	5.40%	4.05%	2.70%	1.35%	0.00%	-1.35%	-2.70%	-4.05%	-5.40%
High Energy (Positive)	3.11%	2.33%	1.56%	0.78%	0.00%	-0.78%	-1.56%	-2.33%	-3.11%
High Energy (Negative)	3.60%	2.70%	1.80%	0.90%	0.00%	-0.90%	-1.80%	-2.70%	-3.60%

Not only does the coating variation affect electrode porosity and cell matching ratio, but also the resulting cell capacity. The percentage range of capacity variation resulting from coating tolerance is highly dependent on target loading. Based solely on positive electrode active material loading, the areal capacity change corresponding to $\pm 0.4 \mu\text{m}$ loading tolerance is $\pm 4.0\%$, $\pm 2.0\%$ and $\pm 1.3\%$ for high power/low energy, mid-range, and high energy/low power loadings, respectively.

3.3. “Worst Case Scenario”—Combination of Coating and Calender Tolerance

Performing analysis on coating and calendering processes independently allows for investigation into the greatest impact on electrode physical parameters, allowing the cell manufacturer to understand this impact and focus on one process at a time to minimize cell-to-cell or lot-to-lot variation. Looking at a realistic process of combining both manufacturing operations, the possible “worst case scenario” results in a larger variation of electrode physical properties. From Equation (3), the resulting porosities of a high power/low energy electrode are shown in Table 7.

Table 7. Porosity range for high power/low energy positive and negative electrodes showing combined.

Coating Variation (mg/cm ²)	Positive Electrode						
	Calender Tolerance (μm)						
	-3.0	-2.0	-1.0	0.0	1.0	2.0	3.0
-0.4	25.8%	28.3%	30.6%	32.8%	34.8%	36.8%	38.6%
-0.3	25.0%	27.5%	29.9%	32.1%	34.2%	36.1%	38.0%
-0.2	24.3%	26.8%	29.2%	31.4%	33.5%	35.5%	37.3%
-0.1	23.5%	26.1%	28.5%	30.7%	32.8%	34.8%	36.7%
0	22.7%	25.3%	27.7%	30.0%	32.1%	34.1%	36.0%
0.1	21.9%	24.6%	27.0%	29.3%	31.5%	33.5%	35.4%
0.2	21.2%	23.8%	26.3%	28.6%	30.8%	32.8%	34.8%
0.3	20.4%	23.1%	25.6%	27.9%	30.1%	32.2%	34.1%
0.4	19.6%	22.3%	24.8%	27.2%	29.4%	31.5%	33.5%
Coating Variation (mg/cm ²)	Negative Electrode						
	Calender Tolerance (μm)						
	-3.0	-2.0	-1.0	0.0	1.0	2.0	3.0
-0.4	40.1%	41.6%	43.0%	44.3%	45.6%	46.8%	48.0%
-0.3	39.0%	40.5%	41.9%	43.2%	44.5%	45.8%	47.0%
-0.2	37.8%	39.3%	40.8%	42.2%	43.5%	44.7%	45.9%
-0.1	36.6%	38.2%	39.7%	41.1%	42.4%	43.7%	44.9%
0	35.5%	37.1%	38.6%	40.0%	41.4%	42.7%	43.9%
0.1	34.3%	35.9%	37.5%	38.9%	40.3%	41.6%	42.9%
0.2	33.2%	34.8%	36.4%	37.8%	39.3%	40.6%	41.9%
0.3	32.0%	33.7%	35.3%	36.8%	38.2%	39.6%	40.9%
0.4	30.8%	32.5%	34.1%	35.7%	37.2%	38.6%	39.9%

For a high power/low energy electrode pair, a large range of porosities are possible from relatively small variations in coating and calendering: 19.6% to 38.6% and 30.8% to 48.0% for a nominal 30% and 40% porosity positive and negative electrode, respectively. This porosity variation in a high power/low energy electrode results in a full saturation electrolyte volume range of 59% to 141% compared to an electrode coated and calendered to the target value. Similar results for a high power/low energy negative electrode as shown with an electrolyte volume range of 72% to 128%. These data also highlight the fact that although there are numerous outcomes which result in the correct porosity, the matching ratio, thickness, and cell capacity will be varied, affecting cell performance.

4. Conclusions

Although physical experimental data are not presented for the theoretical design and resulting variation, it is understood that all manufactured parts, whether in industry or academia, will have an associated deviation from the target value. This variation in the produced parts may be the result of the non-uniformity of laboratory scale calender rolls, or the industrial manufacturing process where parts are presented as having a target value and accepted tolerance range. In either scenario, the produced parts may be deemed acceptable. Progressing forward, the manufacturing tolerance can be reduced through the use of high precision coating and calendering equipment. The reduction in these process tolerances will have a dramatic effect on lithium ion cell electrode porosity and matching ratio consistency, which inevitably affects repeatable cell capacity, cycle life, rate capability, safety, as well as many other important characteristics of lithium ion cells.

A simple look at the electrode manufacturing process and the correlation to electrolyte volume may offer a quick explanation into cell-to-cell or lot-to-lot variation observed in different lithium ion cell manufacturing and quality control processes. While this process was applied to a generic positive and negative electrode formulation at different loadings, the analysis and resulting porosity, void volume, and matching ratio variation calculations can be applied to any electrode manufacturing

process. As electrode design moves toward higher energy designs with a higher percentage of active material or thinner, higher power electrodes, the effect of these variations is increased.

For the selected 93% LCO positive electrode and 92% active carbon negative electrode, a coating tolerance of $\pm 0.4 \text{ mg/cm}^2$ and a calender tolerance of $\pm 3.0 \mu\text{m}$ was used. For the high power/low energy positive and negative electrode target loading of 10 and 5.56 mg/cm^2 , respectively, a porosity range of 19.6% to 38.6% and 30.8% to 48.0% for a nominal 30% and 40% porosity positive and negative electrode is possible. Also shown is an equal area negative to positive cell matching ratio range of 0.98 to 1.23, for a target value of 1.1.

Funding: This research received no external funding.

Acknowledgments: Work has been partially supported by the Penn State Hazleton Research Development Grant.

Conflicts of Interest: The authors declare no conflict of interest.

References

1. Blomgren, G.E. The Development and Future of Lithium Ion Batteries. *J. Electrochem. Soc.* **2017**, *164*, A5019–A5025. [[CrossRef](#)]
2. Manthiram, A. An Outlook on Lithium Ion Battery Technology. *ACS Cent. Sci.* **2017**, *3*, 1063–1069. [[CrossRef](#)] [[PubMed](#)]
3. Deng, D. Li-ion batteries: Basics, progress, and challenges. *Energy Sci. Eng.* **2015**, *3*, 385–418. [[CrossRef](#)]
4. Nitta, N.; Wu, F.; Lee, J.T.; Yushin, G. Li-ion battery materials: Present and future. *Mater. Today* **2015**, *18*, 252–264. [[CrossRef](#)]
5. Berckmans, G.; Messagie, M.; Smekens, J.; Omar, N.; Vanhaverbeke, L.; Van Mierlo, J. Cost Projection of State of the Art Lithium-Ion Batteries for Electric Vehicles Up to 2030. *Energies* **2017**, *10*, 1314. [[CrossRef](#)]
6. Shin, D.; Poncino, M.; Macii, E.; Chang, N. A statistical model of cell-to-cell variation in Li-ion batteries for system-level design. In Proceedings of the International Symposium on Low Power Electronics and Design (ISLPED), Beijing, China, 4–6 September 2013; pp. 94–99.
7. Asif, A.A.; Singh, R. Further Cost Reduction of Battery Manufacturing. *Batteries* **2017**, *3*, 17. [[CrossRef](#)]
8. Singh, M.; Kaiser, J.; Hahn, H. Effect of Porosity on the Thick Electrodes for High Energy Density Lithium Ion Batteries for Stationary Applications. *Batteries* **2016**, *2*, 35. [[CrossRef](#)]
9. Suthar, B.; Northrop, P.W.C.; Rife, D.; Subramanian, V.R. Effect of Porosity, Thickness and Tortuosity on Capacity Fade of Anode. *J. Electrochem. Soc.* **2015**, *162*, A1708–A1717. [[CrossRef](#)]
10. Smekens, J.; Gopalakrishnan, R.; Steen, N.V.; Omar, N.; Hegazy, O.; Hubin, A.; Van Mierlo, J. Influence of Electrode Density on the Performance of Li-Ion Batteries: Experimental and Simulation Results. *Energies* **2016**, *9*, 104. [[CrossRef](#)]
11. Novák, P.; Scheifele, W.; Winter, M.; Haas, O. Graphite electrodes with tailored porosity for rechargeable ion-transfer batteries. *J. Power Sources* **1997**, *68*, 267–270. [[CrossRef](#)]
12. Shim, J.; Striebel, K.A. Effect of electrode density on cycle performance and irreversible capacity loss for natural graphite anode in lithium-ion batteries. *J. Power Sources* **2003**, *119*–*121*, 934–937. [[CrossRef](#)]
13. Son, B.; Ryou, M.-H.; Choi, J.; Kim, S.-H.; Ko, J.M.; Lee, Y.M. Effect of cathode/anode area ratio on electrochemical performance of lithium-ion batteries. *J. Power Sources* **2013**, *243*, 641–647. [[CrossRef](#)]
14. Xue, R.; Huang, H.; Li, G.; Chen, L. Effect of cathode/anode mass ratio in lithium-ion secondary cells. *J. Power Sources* **1995**, *55*, 111–114. [[CrossRef](#)]
15. Kim, C.S.; Jeong, K.M.; Kim, K.; Yi, C.W. Effects of capacity ratios between anode and cathode on electrochemical properties for lithium polymer batteries. *Electrochim. Acta* **2015**, *155*, 431–436. [[CrossRef](#)]
16. An, S.J.; Li, J.; Mohanty, D.; Daniel, C.; Polzin, B.J.; Croy, J.R.; Trask, S.E.; Wood, D.L. Correlation of Electrolyte Volume and Electrochemical Performance in Lithium-Ion Pouch Cells with Graphite Anodes and NMC532 Cathodes. *J. Electrochem. Soc.* **2017**, *164*, A1195–A1202. [[CrossRef](#)]
17. Kang, S.-J.; Yu, S.; Lee, C.; Yang, D.; Lee, H. Effects of electrolyte-volume-to-electrode-area ratio on redox behaviors of graphite anodes for lithium-ion batteries. *Electrochim. Acta* **2014**, *141*, 367–373. [[CrossRef](#)]

18. Nanjundaswamy, K.S.; Friend, H.D.; Kelly, C.O.; Standlee, D.J.; Higgins, R.L. Electrode fabrication for Li-ion: Processing, formulations and defects during coating. In Proceedings of the IECEC-97 Thirty-Second Intersociety Energy Conversion Engineering Conference (Cat. No.97CH6203), Honolulu, HI, USA, 27 July–1 August 1997; Volume 1, pp. 42–45.
19. Repp, S.; Harputlu, E.; Gurgen, S.; Castellano, M.; Kremer, N.; Pompe, N.; Wörner, J.; Hoffmann, A.; Thomann, R.; Emen, F.M.; et al. Synergetic effects of Fe ³⁺ doped spinel Li₄ Ti₅ O₁₂ nanoparticles on reduced graphene oxide for high surface electrode hybrid supercapacitors. *Nanoscale* **2018**, *10*, 1877–1884. [CrossRef] [PubMed]
20. Genc, R.; Alas, M.O.; Harputlu, E.; Repp, S.; Kremer, N.; Castellano, M.; Colak, S.G.; Ocakoglu, K.; Erdem, E. High-Capacitance Hybrid Supercapacitor Based on Multi-Colored Fluorescent Carbon-Dots. *Sci. Rep.* **2017**, *7*, 1–13. [CrossRef] [PubMed]
21. Lain, M.J.; Brandon, J.; Kendrick, E. Design Strategies for High Power vs. High Energy Lithium Ion Cells. *Batteries* **2019**, *5*, 64. [CrossRef]



© 2020 by the author. Licensee MDPI, Basel, Switzerland. This article is an open access article distributed under the terms and conditions of the Creative Commons Attribution (CC BY) license (<http://creativecommons.org/licenses/by/4.0/>).